

## RARE SEMILEPTONIC BEAUTY DECAYS IN ATLAS\*

A. POLICICCHIO, G. CROSETTI

University of Calabria and INFN Cosenza  
Via P. Bucci, 87036 Arcavacata di Rende, Rende, Italy

*(Received November 15, 2006)*

We discuss the latest studies on rare semileptonic decays of  $B$ -mesons and  $\Lambda_b$  at the ATLAS detector.

PACS numbers: 13.30.Ce

**1. Introduction**

Rare  $B$ -decays, produced by  $b \rightarrow s, d$  quark FCNC transitions, are forbidden at the tree level in the Standard Model (SM). These decays occur at the lowest order only through one-loop “penguin” and “box” diagrams. The branching ratios of these decays are very small: from  $4 \times 10^{-5}$  for rare radiative decay  $B_d^0 \rightarrow K^* \gamma$  to  $10^{-15}$  for rare Cabibbo suppressed leptonic decay  $B_d^0 \rightarrow e^+ e^-$ .

Careful investigation of rare  $B$ -decays is mandatory for testing ground of the Standard Model and offer a complementary strategy in the search of new physics by probing the indirect effects of new interactions in higher order processes. The probing of loop-induced couplings provides a means of testing the detailed structure of the SM at the level of radiative corrections. In particular, FCNC involving  $b \rightarrow s, d$  transitions, provide an excellent probe of new indirect effects by yielding informations on the masses and coupling of the virtual particles running in the loops. This explains the attention they have received in recent years. The study of such decays gives also other opportunities: to find the values of  $|V_{ts}|$  and  $|V_{td}|$  CKM matrix elements and to provide new informations on long-distance QCD effects in matrix elements of the tensor current.

In the last years the  $B$ -factories BaBar and Belle presented the first results for  $B \rightarrow (K^*, K) l^+ l^-$  branching ratios and forward-backward asymmetry ( $A_{FB}$ ) in these rare semileptonic decays [6–8]. The experimental

---

\* Presented at the “Physics at LHC” Conference, Kraków, Poland, July 3–8, 2006.

branching ratio values are consistent with SM predictions. More precise measurements are needed for differential dimuon invariant mass and forward-backward asymmetry distributions, in order to discriminate between SM and new physics predictions.

In this report we will pay attention to the semileptonic decays with  $\mu^+\mu^-$  pair in final state. We discuss the latest simulation results at ATLAS detector. The branching ratios in SM of these decays can be found in Table I.

TABLE I

Branching ratios in SM of rare  $B$ -decays with  $\mu^+\mu^-$  pair in final states.

Decay channel	BR ratio	Ref.	Form factors	Wilson coeff.
$B^+ \rightarrow K^+\mu^+\mu^-$	$3.5 \times 10^{-7}$	[1]	QCD LCSR	NNLO
$\Lambda_b \rightarrow \Lambda\mu^+\mu^-$	$2.0 \times 10^{-6}$	[2, 3]	HQET	NLO
$B_d^0 \rightarrow K^{0*}\mu^+\mu^-$	$1.3 \times 10^{-6}$	[4, 5]	Quark Model	NLO
$B_s^0 \rightarrow \phi\mu^+\mu^-$	$\sim 10^{-6}$	[4, 5]	Quark Model	NLO

## 2. Theoretical description

From the theoretical point of view, the  $b \rightarrow q$  ( $q = s, d$ ) transitions are described using the effective Hamiltonian

$$\mathcal{H}_{\text{eff}} = -4 \frac{G_F}{\sqrt{2}} V_{tb} V_{tq}^* \sum_{i=1}^{10} C_i(\mu) O_i(\mu) \quad (1)$$

in the form of Wilson expansion (see *e.g.* [9]). The set of Wilson coefficients  $C_i(\mu)$  depends on the current model and contains the lowest order model contributions and perturbative QCD corrections. The scale parameter  $\mu$  is approximately equal to the mass of  $b$ -quark ( $\sim 5$  GeV). This parameter separates the perturbative and nonperturbative contributions of the string interactions. The nonperturbative contribution is contained in the matrix elements of basis operators  $O_i(\mu)$  between the initial and final hadronic states. For the calculation of these matrix elements it is necessary to use different decay-specific nonperturbative methods: QCD Sum Rules, Heavy Quarks Effective Theory, Quark Models and Lattice calculations. The accuracy in nonperturbative calculations depends on a method, but it is not better than 15%. The accuracy of the Wilson coefficient for with NLO and NNLO QCD corrections [10] is not worse than 15% if  $\mu$  parameter ranges in  $[m_b/2, 2m_b]$ .

### 3. ATLAS muon trigger strategy

At the start up, the target peak luminosity for the LHC is  $2 \times 10^{33} \text{ cm}^{-2} \text{ s}^{-1}$ , rising to the full design luminosity of  $10^{34} \text{ cm}^{-2} \text{ s}^{-1}$  after a few years of running. There will be an average of 4.6 and 23 interactions per bunch crossing for initial and design luminosity, respectively. About 1% of collisions will produce a  $b\bar{b}$  pair. The challenge for the trigger is to select those events of most interest for the ATLAS  $B$ -Physics program [11], within the limited trigger and storage resources available. The ATLAS  $B$ -Physics trigger [12, 13] is based on a lepton signature at the first level, which can be accompanied by additional, lower transverse energy signature of leptons and jets. These signatures are refined in the higher trigger levels where specific decays are reconstructed.

For semileptonic dimuon decays, the trigger will be limited to a dimuon trigger. This is based on the detection of two muons found in the first trigger level with a transverse momentum ( $p_T$ ) threshold of 6 GeV and 4 GeV, respectively. At the second level, the muon  $p_T$  measurements will be confirmed in the muon precision chambers, the tile calorimeter and then extrapolated to the Inner Detector in order to reject muons from  $\pi/K$  decays. At the Event Filter level, offline track quality reconstruction, vertex and mass cuts will be applied to select candidates for specific exclusive or semi-inclusive decays such as  $J/\Psi \rightarrow \mu^+ \mu^-$  and  $B \rightarrow \mu^+ \mu^- (X)$ . This strategy can be used at low initial luminosity and also at nominal LHC  $10^{34} \text{ cm}^{-2} \text{ s}^{-1}$  luminosity.

### 4. Data samples

A series of Monte Carlo data production, called Data Challenge (DC), has started in 2002. Their aim is the validation of the computing and software models. They also provide large data samples for the preparation of the physics analysis. The data sample for the present studies have been produced in the framework of the DC2 production, using the final ATLAS detector layout, simulation based on Geant4 and new GRID-oriented software [14–16].

Below we introduce the basic results of the data analysis. The main theoretical modelling basis for Monte Carlo generation of data samples is shown in Table I. Pythia [17] and Evtgen [18] Monte Carlo software packages have been used in the framework of ATLAS software for data production. The first level trigger cuts on muons and Inner Detector acceptance cuts pseudorapidity ( $|\eta| < 2.5$  and  $p_T > 0.5 \text{ GeV}$ ) on stable hadrons and muons have been applied at the generation level for all the decay channels. The number of events expected for semileptonic dimuon decay channel after trigger and acceptance cuts (triggerable and reconstructible) events is shown in Table II for  $30 \text{ fb}^{-1}$  integrated luminosity (3 years at  $10^{33} \text{ cm}^{-2} \text{ s}^{-1}$ ).

TABLE II

Number of expected events in  $30 \text{ fb}^{-1}$  integrated luminosity after first level trigger and Inner Detector acceptance cuts.

Decay channel	BR ratio	Events in $30 \text{ fb}^{-1}$
$B^+ \rightarrow K^+ \mu^+ \mu^-$	$3.5 \times 10^{-7}$	40000
$\Lambda_b \rightarrow \Lambda \mu^+ \mu^-$	$2.0 \times 10^{-6}$	28000
$B_d^0 \rightarrow K^{0*} \mu^+ \mu^-$	$1.3 \times 10^{-6}$	120000
$B_s^0 \rightarrow \phi \mu^+ \mu^-$	$\sim 10^{-6}$	21000

The impact of trigger and acceptance cuts has been studied for  $\Lambda_b \rightarrow \Lambda \mu^+ \mu^-$  channel. Trigger cuts slightly prefer higher dimuon invariant mass and a slight suppression of  $|A_{\text{FB}}|$  in low  $q^2/M_{\Lambda_b}^2$  region has been found, but they do not change significantly the dimuon invariant mass and the forward-backward asymmetry differential distributions. We have to point out that these distributions are very sensitive to SM extensions.

#### 4.1. Background samples

The semileptonic decay channel with  $c\bar{c}$  resonances ( $J/\Psi$  and  $\Psi(2S)$ ) decaying into two muons represent an irreducible background source for rare decays. Only a cut on dimuon invariant mass around mass peaks can remove it.  $B^+ \rightarrow K^+ J/\Psi(\mu^+ \mu^-)$  and  $B^+ \rightarrow K^+ \Psi(2S)(\mu^+ \mu^-)$  data sample have been fully simulated and reconstructed in order to evaluate the resonances mass width. Semileptonic decays of both  $b$  and  $\bar{b}$  quarks and double semileptonic decays of  $b$  quarks ( $b \rightarrow c\mu\nu$ ,  $c \rightarrow s\mu\nu$ ) can be a combinatorial background source for rare semileptonic decays. A bulk of  $b\bar{b} \rightarrow \mu^+ \mu^- X$  events with muons and hadrons satisfying the trigger and acceptance cuts have been produced in order to evaluate combinatorial background events after reconstruction cuts. Other specific decays channels can represent background sources for the decay channel under investigation. In particular kaons and pions misidentification as muons can generate background events. In the current studies these decay channels have been not included.

## 5. Simulation of rare semileptonic $B$ -decays

### 5.1. $B^+ \rightarrow K^+ \mu^+ \mu^-$ decay

For  $B^+ \rightarrow K^+ \mu^+ \mu^-$  decay, the  $A_{\text{FB}}$  vanishes in all the dimuon invariant mass spectrum in the SM framework. Non zero values for  $A_{\text{FB}}$  are predicted in some beyond SM theories [20, 21]. The forward–backward asymmetry is defined as

$$A_{\text{FB}}(\hat{s}) = \frac{\int_0^1 \frac{d\Gamma}{d\hat{s}\hat{z}} d\hat{z} - \int_{-1}^0 \frac{d\Gamma}{d\hat{s}\hat{z}} d\hat{z}}{\int_{-1}^1 \frac{d\Gamma}{d\hat{s}\hat{z}} d\hat{z}}, \quad (2)$$

where  $\hat{z} = \cos \theta$  ( $\theta$  is the angle between  $\mu^+$  and  $K^+$  in the  $\mu^+ \mu^-$  rest frame) and  $\hat{s} = (p_{\mu^+} + p_{\mu^-})^2 / M_{\Lambda_b}^2 = q^2 / M_{\Lambda_b}^2$  is the dimuon invariant mass.

After trigger and offline analysis cuts and considering a 75% first level trigger efficiency, 1500 signal events are expected in  $30 \text{ fb}^{-1}$  integrated luminosity. Due to limited statistics of simulated background events available, only an upper limit of 10000 background events was determined. These results will be soon updated. The simulation shows that the trigger and the offline cuts do not change the shape of the dimuon mass spectrum and  $A_{\text{FB}}$  distribution, as shown in Fig. 1.

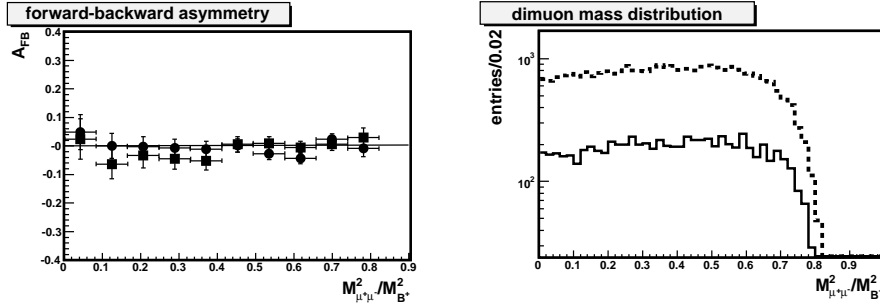


Fig. 1. Dimuon mass spectrum and  $A_{\text{FB}}$  distribution after trigger and offline analysis cuts for  $B^+ \rightarrow K^+ \mu^+ \mu^-$  decay. In dimuon mass spectrum, the dotted and continuous lines represent respectively events at the generation level and after analysis cuts on reconstructed events. In the  $A_{\text{FB}}$  distribution, the circular and the squared points are events at the generation level and events after analysis cuts respectively.

In Fig. 2(a) the  $A_{\text{FB}}$  distribution is presented. The point in red are the experimental Belle collaboration measurements [7] while the point in blue are the ATLAS expected measurements after  $30 \text{ fb}^{-1}$  integrated luminosity. ATLAS will give an important contribution to  $A_{\text{FB}}$  measurements.

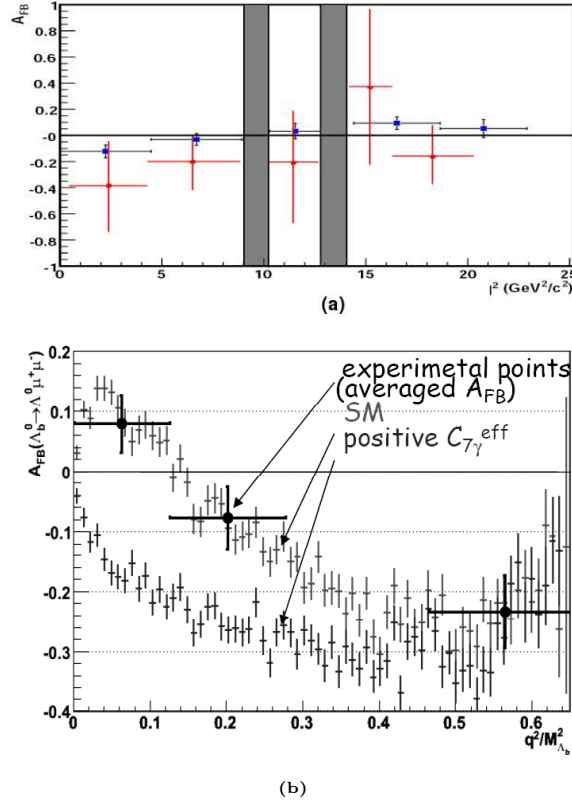


Fig. 2. Forward-backward asymmetry for (a)  $B^+ \rightarrow K^+ \mu^+ \mu^-$  decay (see Sec. 5.1) and (b)  $\Lambda_b \rightarrow \Lambda \mu^+ \mu^-$  decay (see Sec. 5.2).

### 5.2. $\Lambda_b \rightarrow \Lambda \mu^+ \mu^-$ decay

For  $\Lambda_b \rightarrow \Lambda \mu^+ \mu^-$  decay, the  $A_{FB}$  is very sensitive to SUSY both for small and large value of dimuon invariant mass. After trigger and offline analysis cuts and considering a 75% first level trigger efficiency, for  $30 \text{ fb}^{-1}$  about 800 signal and 4000 upper limit background events are expected. The dimuon invariant mass  $q^2/M_{\Lambda_b}^2$  is divided into three region intervals: the first interval is from  $(2m_\mu/M_{\Lambda_b})$  to the zero-point, the second interval is from the zero-point to lower boundaries of  $c\bar{c}$  resonances and the last is from resonances area to  $(M_{\Lambda_b} - M_\Lambda)^2/M_{\Lambda_b}^2$ . The results are shown in Fig. 2(b). Upper point set corresponds to the theoretical SM predictions [2] and the lower set corresponds to one of the possible non-SM prediction [3]. ATLAS will be able to separate SM from some of its extensions with high confidence level.

### 5.3. $B_d^0 \rightarrow K^{0*} \mu^+ \mu^-$ and $B_s^0 \rightarrow \phi \mu^+ \mu^-$ decays

The branching ratios and the  $A_{\text{FB}}$  differential distributions of such semileptonic decays are very sensitive to SM extensions. After trigger and offline analysis cuts and considering a 75% first level trigger efficiency, we expect about 2500 signal events for  $B_d^0 \rightarrow K^{0*} \mu^+ \mu^-$  and 900 signal events for  $B_s^0 \rightarrow \phi \mu^+ \mu^-$  after  $30 \text{ fb}^{-1}$  integrated luminosity. A upper limits of 10000 events were determined for background events for both decays. In Fig. 3 the  $A_{\text{FB}}$  is presented for  $B_d^0 \rightarrow K^{0*} \mu^+ \mu^-$  decay. Solid line corresponds to SM predictions, according to [4]. Dashed and dotted lines are boundaries for MSSM predictions [19]. The points in black with large error bars are the experimental Belle collaboration measurements [6] and the points with small error bars the ATLAS expected measurements after  $30 \text{ fb}^{-1}$ . The bars in abscissa coordinate represent the kinematic intervals and the  $c\bar{c}$  resonances kinematic area have been excluded. We can see, it will be enough statistic after 3 years of LHC operations for SM confirmation and setting strong limits on SM extensions or registration of beyond SM contributions.

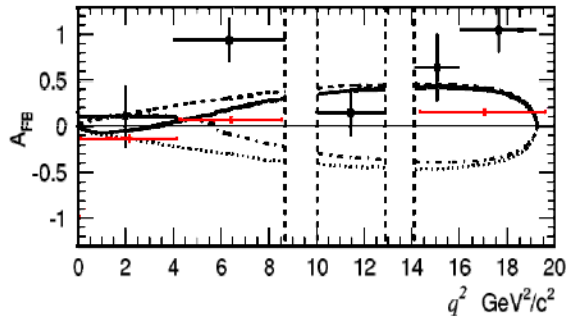


Fig. 3. Forward-backward asymmetry for  $B_d^0 \rightarrow K^{0*} \mu^+ \mu^-$  decay (see Sec. 5.3).

## 6. Conclusions

A full simulation of rare semimuonic  $B$ -decays for ATLAS detector with realistic final detector layout has been performed. The corresponding background has been simulated, although more statistics is needed and some specific background sources have yet to be included. In Table III the number of events expected after  $30 \text{ fb}^{-1}$  integrated luminosity for the semileptonic dimuon decay channels is shown. Also the number of background events and the signal reconstruction efficiency have been reported. The simulation studies show that ATLAS detector will be capable to extract signals of all rare semimuonic  $B$ -decays investigated until now and achieve the sensitivity allowing to identify presence of the SUSY contributions.

TABLE III

Number of expected signal and background events in  $30 \text{ fb}^{-1}$  integrated luminosity and signal reconstruction efficiency.

Decay channel	Signal eff.	Expected signal events	Expected BG events
$B^+ \rightarrow K^+ \mu^+ \mu^-$	0.05	1500	$< 10000$
$\Lambda_b \rightarrow \Lambda \mu^+ \mu^-$	0.038	800	$< 4000$
$B_d^0 \rightarrow K^{0*} \mu^+ \mu^-$	0.03	2500	$< 10000$
$B_s^0 \rightarrow \phi \mu^+ \mu^-$	0.04	900	$< 10000$

## REFERENCES

- [1] A. Ali *et al.*, *Phys. Rev.* **D66**, 034002 (2002).
- [2] C.H. Chen *et al.*, *Phys. Rev.* **D64**, 074001 (2001).
- [3] T.M. Aliev *et al.*, *Nucl. Phys.* **B649**, 168 (2003).
- [4] D. Melikhov *et al.*, *Phys. Rev.* **D57**, 6814 (1998).
- [5] D. Melikhov *et al.*, *Phys. Rev.* **D62** 014006, (2000).
- [6] A. Ishikawa *et al.* (Belle Collaboration), *Phys. Rev. Lett.* **96**, 251801 (2006).
- [7] K. Abe *et al.* (Belle Collaboration), [hep-ex/0410006](#).
- [8] B. Aubert *et al.* (BaBar Collaboration), *Phys. Rev.* **D73**, 092001 (2006).
- [9] G. Buchalla *et al.*, *Rev. Mod. Phys.* **68**, 1125 (1996).
- [10] C. Bobeth *et al.*, *Nucl. Phys.* **B574**, 291 (2000).
- [11] ATLAS Collaboration, ATLAS Detector and Physics Performance Technical Design Report, CERN/LHCC/99-15 (1999).
- [12] J. Baines *et al.*, ATL-DAQ-COM 2002-013.
- [13] M. Smizănská, *Eur. Phys. J.* **C34**, 385 (2004).
- [14] D. Adams *et al.*, ATL-SOFT-2004-007, (2005).
- [15] LCG Project Collaboration, CERN-LHCC-2005-024, (2005).
- [16] ATLAS Collaboration,  
[http://atlas.web.cern.ch/Atlas/GROUPS/Software/00/architecture/General/Tech.Doc/Manual/2.0.0\\_DRAFT/AthenaUserGuide/pdf](http://atlas.web.cern.ch/Atlas/GROUPS/Software/00/architecture/General/Tech.Doc/Manual/2.0.0_DRAFT/AthenaUserGuide/pdf).
- [17] M. Smizănská, ATL-COM-PHYS-2003-038, (2003).
- [18] M. Smizănská, J. Catmore, ATL-COM-PHYS-2004-041, (2004).
- [19] P. Cho *et al.*, *Phys. Rev.* **D54**, 3329 (1996).
- [20] Qi-Shu Yan *et al.*, *Phys. Rev.* **D62**, 094023 (2000) [[hep-ph/0004262](#)].
- [21] C. Bobeth *et al.*, *Phys. Rev.* **D64**, 074014 (2001) [[hep-ph/0104284](#)].